

## New Polymers Based on 2,6-di(thiophen-2-yl)aniline and 2,2'-(thiophen-2,5-diyl)dianiline Monomers. Preparation, Characterization and Thermal, Optical, Electronic and Photovoltaic Properties.

I. A. Jessop<sup>1,\*</sup>, P.P. Zamora<sup>1</sup>, F.R. Diaz<sup>1</sup>, M.A. del Valle<sup>2</sup>, A. Leiva<sup>3</sup>, L. Cattin<sup>4</sup>, M. Makha<sup>5,6</sup>, J. C. Bernède<sup>5</sup>

<sup>1</sup> Pontificia Universidad Católica de Chile, Facultad de Química, Departamento de Química Orgánica, Laboratorio de Polímeros, Av. Vicuña Mackenna 4860, Santiago de Chile

<sup>2</sup> Pontificia Universidad Católica de Chile, Facultad de Química, Departamento de Química Inorgánica, Laboratorio de Electroquímica de Polímeros, Av. Vicuña Mackenna 4860, Santiago de Chile

<sup>3</sup> Pontificia Universidad Católica de Chile, Facultad de Química, Departamento de Química Física, Av. Vicuña Mackenna 4860, Santiago de Chile

<sup>4</sup> Université de Nantes, Institut des Matériaux Jean Rouxel (IMN), CNRS, UMR 6205, 2 rue de la Houssinière, BP 32229, 44322 Nantes cedex 3, France

<sup>5</sup> Université de Nantes, MOLTECH-Anjou, CNRS, UMR 6200, 2 rue de la Houssinière, BP 92208, Nantes, F-44000 France

<sup>6</sup> Laboratoire Optoélectronique et Physico-chimie des Matériaux, unité de recherche associé au CNRST-URAC-14-Université Ibn Tofail, Faculté des Sciences BP 133 Kenitra 14000, Morocco

\*E-mail: [iajessop@uc.cl](mailto:iajessop@uc.cl)

Received: 9 August 2012 / Accepted: 12 September 2012 / Published: 1 October 2012

---

A new series of polymers, chemically and electrochemically obtained from monomers containing aniline and thiophene moieties, has been prepared. The purpose is to use them as electron donor layers in the fabrication of dual-layer organic solar cells. Both the monomers and the polymers were characterized using techniques such as NMR, FT-IR, cyclic voltammetry, etc. It was found that polymer growth occurred only through aniline unit(s) and not through thiophene unit(s), as might also be expected. Optical and electronic studies revealed that the products displayed properties suitable for use in photovoltaic devices. However, prepared prototypes yields ranged just between  $10^{-2}$  and  $10^{-3}$ .

---

**Keywords:** conducting polymers, aniline and thiophene derivatives, chemical polymerization, electrochemical polymerization, photovoltaic devices.

## 1. INTRODUCTION

A polymer is defined as suitable for electronic applications if a reasonable electrical conductivity is provided in its doped state, as well as good reversibility of the doping/undoping processes, high stability, i.e. evidencing no chemical decomposition due to solvent or other agents, and mechanical properties that allow easy handling. However, a material that meets all these characteristics has not yet been prepared. That is one of the reasons why conducting polymers have attracted so much attention over the past 30 years.

Among the intrinsically conductive organic polymers, polyaniline (PANI) and its derivatives are, to date, the most widely used materials [1]. Its high stability, unique electrochemical properties, low cost and easy preparation, offer a wide variety of applications [2-9]. However, despite synthesis conditions being repeatedly optimized, its conductivity remains low in comparison with other semiconducting polymers such as polyacetylene and polypyrrole.

On the other hand, polythiophene (PTh) is quite similar to PANI in connexion with its high thermal and atmospheric stability, good solubility, ease of processing and high conductivity when doped, consequently it has also been used in a variety of technological applications [10-13].

Chemical and electrochemical polymerization of aniline with thiophene has been found in the literature. The results showed that the obtained intermediate properties, e.g. electrical conductivity and solubility, are very promising for application in photocells [14-16]. All this has led us to postulate that it is possible to improve the properties of these polymers by designing monomers containing units of both compounds, affording thus hybrid precursors.

To test this hypothesis, in the current work two new monomers containing aniline and thiophene units were first synthesized and characterized. Subsequently their respective polymers, chemically and electrochemically prepared, were spectroscopic, thermal, optical and electronically characterized. In addition, they were evaluated as electron donor materials in dual-layer organic solar cells.

## 2. EXPERIMENTAL DETAILS

The chemicals used in this study were purchased from Sigma-Aldrich Co., except for Pd[PPh<sub>3</sub>]<sub>2</sub>Cl<sub>2</sub> and solvents purchased from Merck & Co. 2-(4,4,5,5-tetramethyl-1,3,2-dioxaborolan-2-yl)aniline was prepared according to Baldwin et al. [17] (yield 70%).

NMR spectra were recorded on a Bruker 400 MHz spectrophotometer. FT-IR spectra were run on a Bruker, model Vector 22, using KBr pellets. Elemental analysis was performed on a Fisons analyzer Model EA-1108. The solubility was also determined in various organic solvents, e.g. DMSO, NMP, THF, CHCl<sub>3</sub>, etc. Thermogravimetric analysis (TGA) was carried out on a Mettler TA-3000 Thermal Analysis System equipped with a TC-10A processor and a TG-50 thermobalance with a Mettler MT5 microbalance, heating the samples from 25 to 900 °C at a rate 10 °C min<sup>-1</sup> under nitrogen atmosphere. The glass transition temperature (T<sub>g</sub>) was measured using differential scanning calorimetry (DSC) technique on a Mettler-Toledo DSC 821 calorimetric system, to perform heating processes at 20 °C min<sup>-1</sup> under nitrogen from -100 to 110 °C, in the first instance, and then between 25

and 300 °C for subsequent cycles. UV-Vis spectra were obtained on a SPECORD 40 Analytik Jena spectrophotometer using 1 cm optical path quartz cells. Electrochemical studies were performed on a BAS CV-50W Voltmaster using cyclic voltammetry. Electrochemical measurements were accomplished in an anchor-type three-compartment cell. A 0.07 cm<sup>2</sup> geometric area platinum disk and a Pt coil of large surface area were used as working and counter electrode, respectively. Ag/AgCl in tetramethylammonium chloride, whose potential matches that of a saturated calomel electrode at room temperature, was used as reference electrode [18]. Unless otherwise stated all potential quoted in the current work are referred to this electrode. Prior to each measurement, the working solution was flushed with high purity argon for 15-20 minutes. An inert atmosphere was maintained over the solution throughout the experiment. The working solution was made up of 1·10<sup>-3</sup> mol L<sup>-1</sup> monomer and 1·10<sup>-2</sup> mol L<sup>-1</sup> tetrabutylammonium hexafluorophosphate (TBAHFP) as supporting electrolyte in acetonitrile as solvent. Finally, the photovoltaic device prototype was assembled according to the following scheme: Indium-tin oxide (ITO) coated glass anode/anode buffer layer (MoO<sub>3</sub>)/ undoped electron donor polymer (our materials)/electron acceptor material (Fullerene C<sub>60</sub>)/exciton blocking layer (aluminum (8-(tris-hydroxyquinolato) Alq<sub>3</sub>)/aluminum cathode. The layers were deposited on ITO by sublimation at 1·10<sup>-7</sup> atm. The thickness and deposition rate of the films was estimated in situ by a quartz monitor. The electrical characterization of the devices was conducted using an automated I-V tester in the presence and absence of sunlight determined with a solar simulator (Oriel 300 W) calibrated at a 100 mW/cm<sup>-2</sup> light intensity.

## 2.1. Monomers synthesis

The monomers were synthesized via Suzuki-Miyaura cross-coupling reaction [19] according to the procedure described by Bryce et al. [20].

### 2.1.1. 2,6-di(thiophen-2-yl)aniline (MonA)

0.502 g (2 mmol) of 2,6-dibromoaniline, 0.210 g (0.3 mmol) of Pd[PPh<sub>3</sub>]<sub>2</sub>Cl<sub>2</sub> and 0.768 g (6 mmol) of 2-thiophenboronic acid were placed into a 100 mL two-neck round-bottom flask, fitted with a reflux condenser. Vacuum and argon filling cycles were performed and finally the system was left with a balloon containing argon. 20 mL of degassed 1,4-dioxane was then added and the mixture was stirred for 30 minutes at room temperature. Subsequently 8 mL aqueous 1 mol L<sup>-1</sup> of K<sub>2</sub>CO<sub>3</sub> (8 mmol) solution was added and the mixture was refluxed for 72 hours. After this period of time, the reaction was allowed to cool at room temperature and next 10 mL of water was added. The flask content was transferred to a separator funnel wherein ethyl acetate EtOAc and a saturated NaCl solution were added followed by the extraction of the organic phase. The latter step was repeated twice. The extracted organic phase was dried over MgSO<sub>4</sub>, filtered through a celite plug and concentrated on a rotary evaporator. The concentrate was passed through a silica gel column using a 95%/5% n-hexane/EtOAc mixture as eluent. Finally, the purified product was concentrated and vacuum dried for

24 hours. 0.489 g (95% yield) of a yellow oil was obtained. The latter was recrystallized from an ethanol/water mixture to give a light yellow solid.

### 2.1.2. 2,2'-(thiophen-2,5-diyl)dianiline (MonB)

A 100 mL two-neck round-bottom flask, fitted with a reflux condenser, was loaded with 0.971 g (4.4 mmol) of 2-(4,4,5,5-tetramethyl-1,3,2-dioxaborolan-2-yl)aniline and 0.154 g (0.2 mmol) of Pd[PPh<sub>3</sub>]<sub>2</sub>Cl<sub>2</sub>. Vacuum and argon filling cycles were performed and finally a balloon containing argon was attached to the system. 0.2 mL (1.8 mmol) of 2,5-dibromothiophene and 20 mL degassed 1,4-dioxane was then added and the mixture stirred for 30 minutes at room temperature. Subsequently 8 mL of aqueous 1 mol L<sup>-1</sup> K<sub>2</sub>CO<sub>3</sub> (8 mmol) was added and the mixture refluxed for 72 hours. The work-up proceeded as described for compound MonA. The product was purified by silica gel column using a 3:1 n-hexane/EtOAc mixture as eluent and allowed drying for 24 hours in a vacuum oven. 0.447 g (95% yield) of a brown solid was obtained.

### 2.2. Polymers synthesis: Poly[2,6-di(thiophen-2-yl)aniline] (PolyA) and Poly[2,2'-(thiophen-2,5-diyl)dianiline] (PolyB)

MonA and MonB were chemically polymerized using the method proposed by Chan et. al. [21] that uses anhydrous FeCl<sub>3</sub> as oxidizing agent and chloroform as solvent. To optimize polymers syntheses to obtain the most conductive state (emeraldine state), the ratio oxidizing-agent mmoles/monomer mmoles was varied as follows: 2:1, 4:1, 6:1 and 8:1. The relative intensities of the quinoid (1600 cm<sup>-1</sup>) and benzenoid (1450 cm<sup>-1</sup>) stretching bands in the infrared spectra, that provide information about the oxidation state of PANI derivatives [22], were analyzed. The 4:1 oxidizing/monomer ratio proved to be the most suitable one.

A 100 mL two-neck round-bottom flask was loaded with 0.257 g (1 mmol) of MonA or 0.266 g (1 mmol) of MonB and 0.649 g (4 mmol) of anhydrous FeCl<sub>3</sub> in 60 mL of anhydrous chloroform. The mixture was stirred in the darkness and inert atmosphere during 24 hours at 5 °C. As for PolyA, a dark precipitate was obtained. The solid was then filtered off and stirred for 48 hours in methanol. As PolyB was more soluble than PolyA, the reaction solvent was evaporated using a rotary evaporator. Once the room temperature was reached, water and acetone were added (the latter with the aim of extracting the oligomeric fractions) and the mixture was then stirred for 48 h. Polymers de-doping was accomplished by filtering the compound and stirring it in a 50% of aqueous hydrazine solution for 24 hours. Finally, the mixtures were filtered again and the solids were dried for 24 hours at 50 °C in a vacuum oven. 0.130 g (yield 51%) of a brown compound (PolyA) and 0.153 g (58% yield) of a black product (PolyB) were obtained.

The electrochemical polymerization was carried out using cyclic voltammetry technique within a potential window previously established as optimal under the experimental conditions employed herein. More details will be explained and discussed in the following section.

### 3. RESULTS AND DISCUSSION

#### 3.1. Monomers characterization

During synthesis optimization thin layer chromatography was utilized for monitoring the reaction progress. This procedure revealed that the limiting reactant was consumed between 36 and 48 h. However, after purification of the compounds at those times, the yields found were low, e.g. below 20% for MonA and less than 40% for MonB. Among the isolated components, products from monocoupling were found. These results led to the conclusion that the coupling of boronic acid or ester with aryl dihalides do not occur in a concerted way, but in two stages, presumably due to the large electronic and steric hindrance presented by the monocoupled-catalyst intermediary when the second aromatic system tries to join it.

##### 2,6-di(thiophen-2-yl)aniline (MonA)

m. p.: 66-64 °C. FT-IR (film,  $\text{cm}^{-1}$ ): 3445-3370 (NH stret.), 3105-3065 (ArC-H stret. and ThC-H stret.), 1605 (ArC-C stret. and NH sci.), 1449 (ArC-C stret.), 1219 (ArC-N stret.), 850 (ThC-C ring stret.), 820 (ArC-H oop. bend. and ThC-H oop. bend.), 788 (ArC-H wag.), 744 (ArC-C and ThC-C ring def.) and 699 (ThC-H oop. bend.).  $^1\text{H}$  NMR (400 MHz,  $\text{CDCl}_3$ ):  $\delta$  7.35 (dd,  $J = 5.2$  and  $1.2$  Hz,  $2\text{H}_F$ ), 7.25 (d,  $J = 7.6$  Hz,  $2\text{H}_C$ ), 7.23 (dd,  $J = 3.5$  and  $1.1$  Hz,  $2\text{H}_D$ ), 7.12 (dd,  $J = 5.1$  and  $3.5$  Hz,  $2\text{H}_E$ ), 6.80 (t,  $J = 7.62$  Hz,  $1\text{H}_B$ ), 4.37 (s,  $2\text{H}_A$ ).  $^{13}\text{C}$  NMR (400 MHz,  $\text{CDCl}_3$ ):  $\delta$  142.7 ( $\text{C}_1$ ), 141.3 ( $2\text{C}_5$ ), 131.4 ( $2\text{C}_8$ ), 128.0 ( $2\text{C}_3$ ), 126.7 ( $2\text{C}_7$ ), 126.0 ( $2\text{C}_6$ ), 120.8 ( $2\text{C}_2$ ), 118.3 ( $\text{C}_4$ ). Elemental analysis calculated for  $\text{C}_{14}\text{H}_{11}\text{NS}_2$  (%): C, 65.33; H, 4.31; N, 5.44; S, 24.92. Found (%): C, 65.21; H, 4.25; N, 5.44; S, 24.17.

##### 2,2'-(thiophen-2,5-diyl)dianiline (MonB)

m. p.: 131-129 °C. FT-IR (film,  $\text{cm}^{-1}$ ): 3445-3350 (N-H stret.), 3195-3020 (ArC-H stret. and ThC-H stret.), 1614 (ArC-C stret. and N-H sci.), 1500-1450 (ArC-C stret., ThC-C stret. and N-H stret.), 1260 (ArC-N stret.), 825 (ArC-H oop. bend. and ThC-C oop. bend.) y 748 (ThC-H oop. bend. and ArC-H wag.).  $^1\text{H}$  NMR (400 MHz,  $\text{CDCl}_3$ ):  $\delta$  7.32 (dd,  $J = 7.6$  and  $1.5$  Hz,  $2\text{H}_E$ ), 7.20 (s,  $2\text{H}_F$ ), 7.15 (td,  $J = 7.9$ ,  $7.7$  and  $1.5$  Hz,  $2\text{H}_C$ ), 6.81 (td,  $J = 7.6$ ,  $7.5$  and  $1.2$  Hz,  $2\text{H}_D$ ), 6.78 (dd,  $J = 8.0$  and  $0.9$  Hz,  $2\text{H}_B$ ), 3.99 (s,  $4\text{H}_A$ ).  $^{13}\text{C}$  NMR (400 MHz,  $\text{CDCl}_3$ ):  $\delta$  144.1 ( $2\text{C}_1$ ), 141.0 ( $2\text{C}_7$ ), 130.9 ( $2\text{C}_3$ ), 129.2 ( $2\text{C}_8$ ), 126.4 ( $2\text{C}_5$ ), 120.0 ( $2\text{C}_6$ ), 118.8 ( $2\text{C}_4$ ), 116.2 ( $2\text{C}_2$ ). Elemental analysis calculated for  $\text{C}_{16}\text{H}_{14}\text{N}_2\text{S}$  (%): C, 72.15; H, 5.30; N, 10.52; S, 12.04. Found (%): C, 71.88; H, 5.64; N, 10.46; S, 13.06.

#### 3.2. Polymers characterization

##### 3.2.1. Infrared Spectroscopy

PolyA and PolyB infrared spectra exhibit a broad band between 3440 and 3450  $\text{cm}^{-1}$ , characteristic of NH polyanilines (PANIs) stretching. Bands corresponding to quinoid (1600  $\text{cm}^{-1}$ ) and

benzenoid ( $1450\text{ cm}^{-1}$ ) stretching where also found. Two medium intensity bands at  $1300$  and  $1250\text{ cm}^{-1}$ , corresponding respectively to aromatic C-N and secondary C-N stretching were observed as well [23]. Figure 2 shows the region between  $900$  and  $650\text{ cm}^{-1}$  for these polymers and their respective monomers. The signal at  $802\text{ cm}^{-1}$  for PolyA and at  $813\text{ cm}^{-1}$  for PolyB, ascribed to out of plane vibration of aniline or anilines rings, are the only one that shifts with respect to monomers signals. This would indicate that the polymers growth occurs just through such unit.

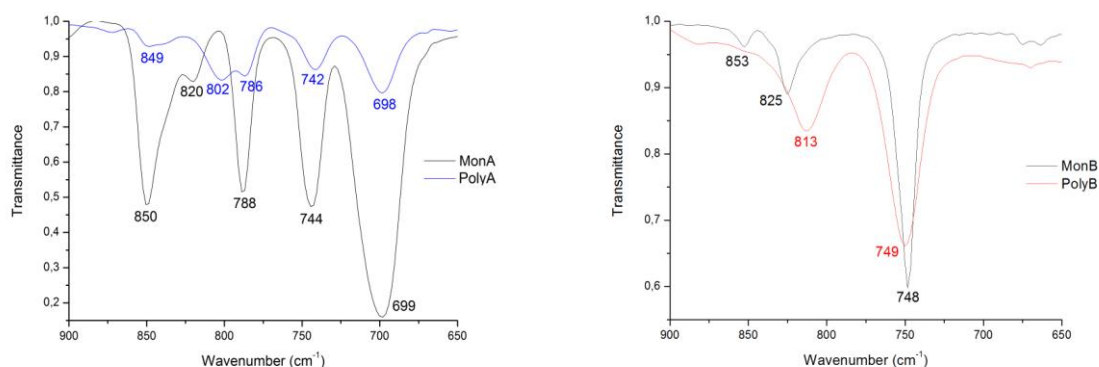


**Figure 2.** IR spectra out of plane vibration region of PolyA and PolyB.

The other bands in this region would be associated to out of plane bendings of the protons in the aniline and thiophene rings, aniline rings waggings and in-plane deformations of the aromatic rings.

### 3.2.2. Solubility

One of the features to be enhanced at the time of synthesizing semiconducting polymers is the solubility. This factor, besides being key for a suitable processability in solution, can directly influence many physical parameters of the polymers, such as crystallinity and microscopic morphology that determines the performance of organic solar cells prepared from them. Table 1 shows the solubility of the studied polymers in various organic solvents.

**Table 1.** Polymers solubility in commonly used organic solvents.

Polymer	Solvent						
	CH <sub>3</sub> CN	CH <sub>3</sub> Cl	DMSO	NMP	DMF	THF	Tol.
PolyA	±	-	±	±	±	-	-
PolyB	-	-	±	±	±	-	-

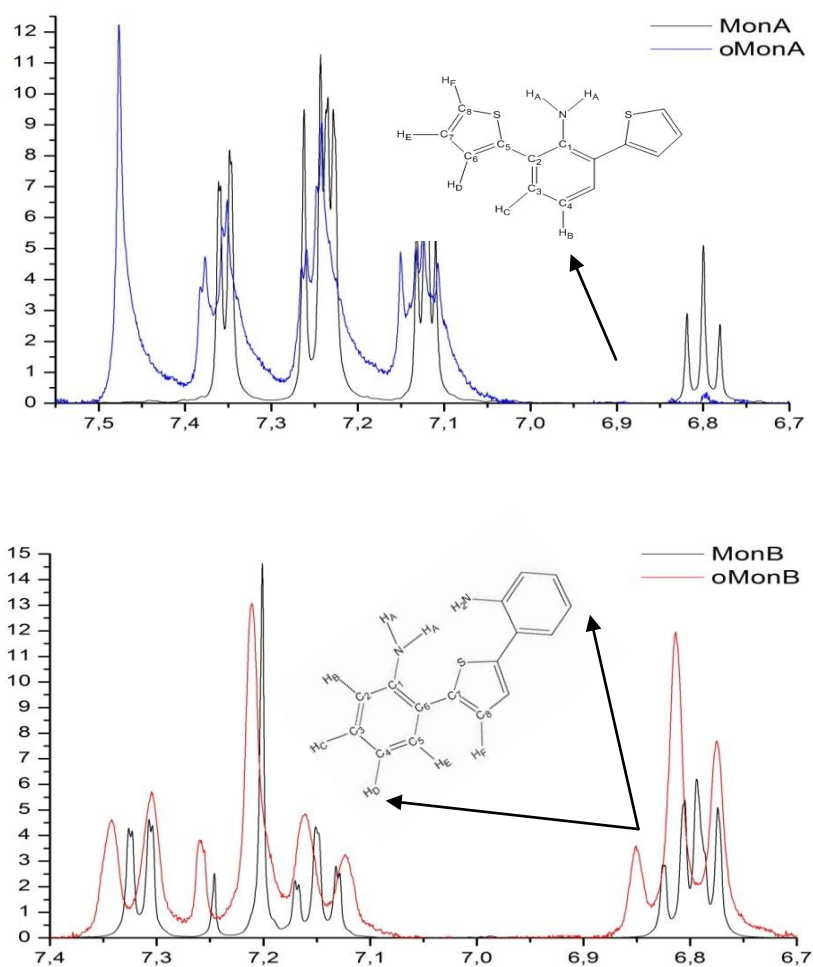
The low solubility of the synthesized polymers can be ascribed to their degree of polymerization and strong intermolecular interactions. It is noteworthy that PANI is soluble in solvents

such as DMF, NMP and DMSO and sparingly soluble in THF and CH<sub>3</sub>Cl [24]. Therefore the presence of one or more thiophene rings that increases the aromatic content of the monomeric unit, would bring about the opposite effect upon solubility of the new products.

As neither PolyA nor PolyB completely dissolved in any of the attempted solvents, their inherent viscosity, that would give an idea of their molecular dimensions, could not be measured.

### 3.2.3. Nuclear Magnetic Resonance

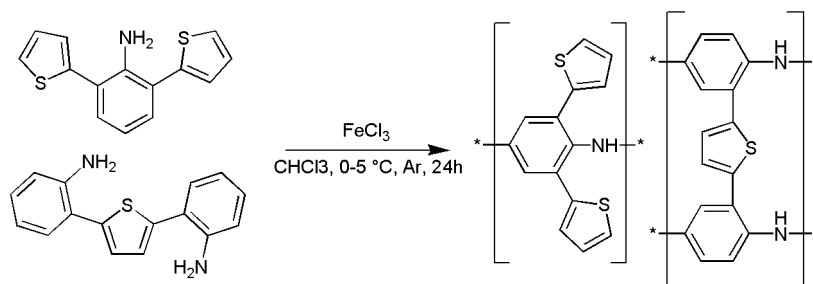
Polymers <sup>1</sup>H-NMR spectra were recorded in DMSO-d<sub>6</sub>, solvent in which they present an intermediate solubility. Interpretation of the fine structure proved to be quite complicated and therefore of little help to understand through which zone or zones of the monomer chains growth takes place. Therefore, the polymerization reaction was carried out for short times (1-2 hours) in order to attain much shorter chains. Figure 3 exhibits MonA (oMonA) and MonB (oMonB) oligomers spectra that proved to be soluble in CD<sub>3</sub>Cl.



**Figure 3.** Enlarged aromatic area of oMonA and oMonB oligomers and their respective monomers <sup>1</sup>H-NMR spectra.

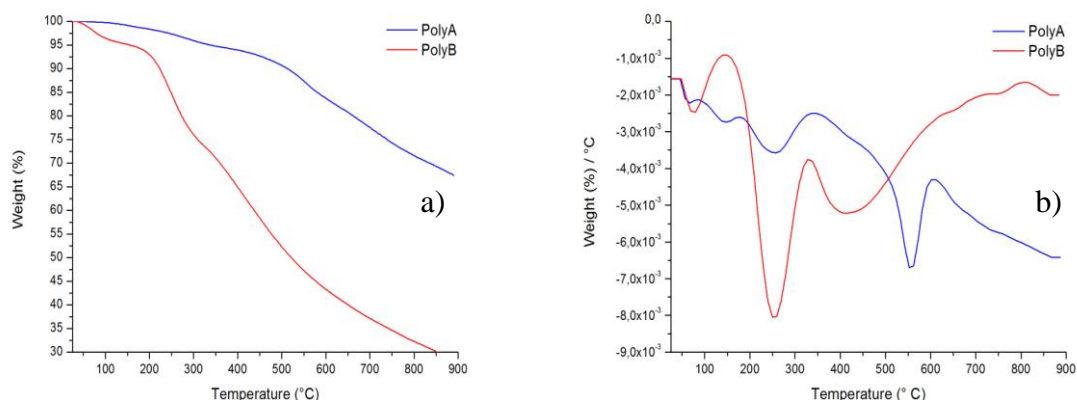
The oMonA spectrum signals present chemical shifts almost identical to that of the corresponding monomer, except for the  $H_B$  triplet, assigned to the proton attached to  $C_4$ , that disappeared. This would corroborate that PolyA growth occurs only through aniline unit. The singlet at 7.47 ppm might correspond to  $H_C$  that shifts to low field as a result of the polymerization process. As for oMonB oligomer, disappearance of the double triplet associated to  $H_D$  proton attached to  $C_4$  is observed. This fact, along with the conversion of the double triplet to double doublet of the  $H_C$  proton and of the double doublet to doublet of the  $H_E$  proton would confirm that PolyB polymer also grows only through aniline units.

From the information provided by the spectroscopic studies, it is assumed the polymerization occurs in the manner shown in Fig. 4.



**Figure 4.** Polymers growth through the aniline unit or units.

### 3.2.4. Thermal studies



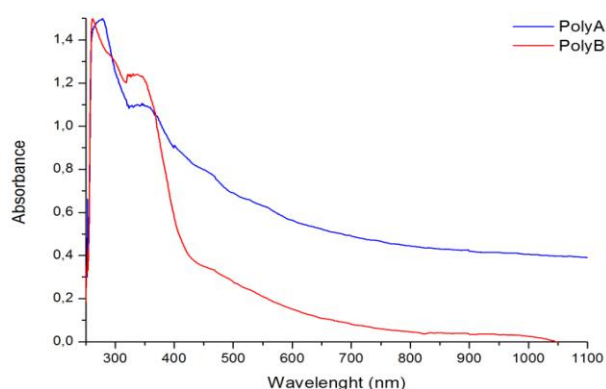
**Figure 5.** PolyA and PolyB TGA curves

Figure 5a shows the thermal degradation profiles obtained by thermogravimetric analysis (TGA) of the synthesized polymers. In general terms, PolyA proved to be more stable than PolyB. PolyB temperature of 50% weight loss is 520 °C. For PolyA this value exceeds 900 °C. Figure 5b shows the differentiate curves of each compound. PolyB and PolyA faster degradation occurred at 253 and 557 °C respectively. These results corroborate that the new polymers were thermally less stable compared to PANI. This may be due to steric hindrance exerted by the side groups in the new

polymers that block the cross-linking process between chains that is known to increase thermal stability [25].

Differential scanning calorimetry (DSC) studies for the second cycle showed a  $T_g$  of about 133 and 117 °C for PolyA and PolyB, respectively. In addition, an exothermic peak centered at 276 °C for PolyA and at 222 °C for PolyB was observed, demonstrating thus the existence of the before mentioned cross-linking process. PANI glass transition temperature  $T_g$ , closely related to the rigidity of the polymer chains, was estimated to be 68 °C [25]. This indicates that side groups addition affects the flexibility of the chain backbone, consistent with the low solubility of the novel synthesized polymers as compared to PANI.

### 3.2.5. UV-Vis spectroscopy



**Figure 6.** UV-Vis spectra of the new polymers with aniline and thiophene units.

Figure 6 shows PolyA and PolyB UV-Vis spectra. As for PolyA, two absorption maxima at 290 and 360 nm attributable respectively to  $\pi$ - $\pi^*$  benzenoid electronic transitions [26] and, presumably, to  $\pi$ - $\pi^*$  thiophene rings electronic transitions [27] can be seen. PolyB presents both maxima described for PolyA plus a third band between 300 and 320 nm, also ascribed to  $\pi$ - $\pi^*$  benzenoid transitions [28]. Intensity of the 370 nm band of both polymers was enhanced with respect to their monomers that, as abovementioned, is ascribed to thiophene rings  $\pi$ - $\pi^*$  electronic transitions. As the polymer growth is not accomplished through these rings, it is assumed this intensity increase might be attributed to a transition between thiophene  $\pi$  orbitals to aniline  $\pi^*$  orbitals. This phenomenon would help to understand why the products growth takes place only through aniline units.

### 3.2.6. Electrochemical study

Various tests were performed for MonA and MonB electro-polymerization by varying the potential window and analyzing the polymer modified electrode in a solution containing only the supporting electrolyte, in order to obtain the most conducting and stable deposit. The chosen working windows were between -1.5 and 1.75 V for PolyA and from -1.5 to 1.45 V for PolyB. The large

amplitude of the working window is because when electrosynthesis is carried out from the equilibrium potential (about 0.2 V), a significant current decreases with increasing cycle number was observed. Cathodic potential scans starting from the equilibrium potential revealed a reversible and stable process that must take place to warrant polymer growth upon the electrode surface. This phenomenon might be ascribed to n-doping and indicated that a significant overpotential was needed to achieve chain growth.

PANI potentiodynamic profile, under the same working conditions, exhibits two anodic processes, namely at 0.2 V, attributable to radical cations formation (conversion of the leucoemeraldine structure to polaronic emeraldine) and at 0.8 V, associated with the appearance of dicationic diradicals (conversion of the emeraldine polaronic structure to a dipolaronic pernigraniline that coexists with the quinoid diimine form) [29-30]. The dicationic diradical acts as an energetic electrophile capable of interacting with a neutral aniline molecule that promotes further polymer growth [31].

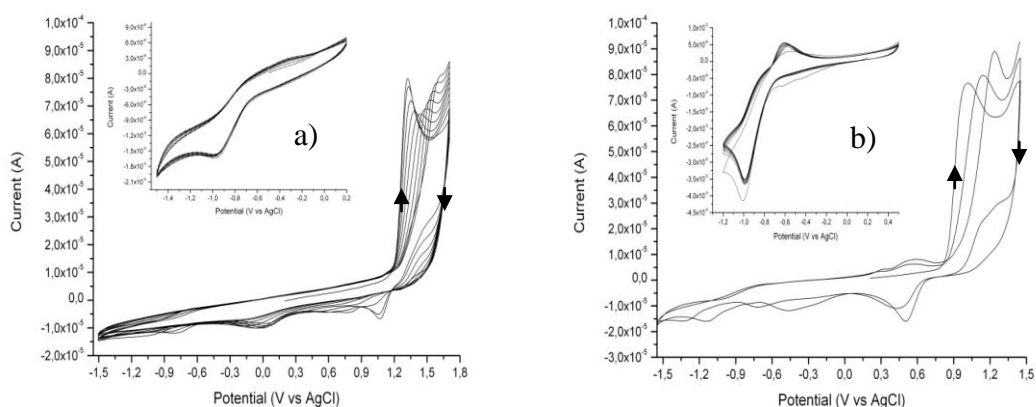


**Figure 7.** PolyA (a) and PolyB (b) voltammetric profiles. Interface Pt |  $1.0 \cdot 10^{-3} \text{ mol L}^{-1}$  monomer +  $1.0 \cdot 10^{-2} \text{ mol L}^{-1}$  HFPTBA,  $\text{CH}_3\text{CN}$ ,  $\nu = 100 \text{ mV s}^{-1}$ . The insert shows an enlargement of the n-doping/undoping process observed at cathodic potentials.

However PolyA profile, Fig. 7, revealed the existence of only one anodic peak, shifted toward more positive potential. This indicates that charge carriers formation is hampered because the side rings are capable of exerting steric hindrance and torsion of the polymeric chain, consistent with the high overpotential required to achieve electro-polymerization. The lack of bipolarons might be due to this fact, or that both anodic peaks would be superimposed, i.e. unresolved. PolyA voltammetric study also showed that the current decreased until the sixth cycle and then started growing. The decrease would indicate that as the polymer is deposited upon the electrode, conjugation and conductivity are been lost, probably due to torsion and interchain interactions that hamper charge carriers to move across the polymer network. The subsequent current increase would be explained considering a re-ordering of the initially formed chains that re-deposit, facilitating interchain charges mobility and growth of new oligomeric chains on the electrode surface.

As for PolyB, two processes, such as for PANI, were observed between 0.3 and 0.7 V, due to polarons formation, and between 0.8 and 1.2 V, ascribed to bipolarons. Voltammetric profile shows that as the number of cycles increases, the current associated to both processes increases too. However, after the third cycle the current begins to decrease, indicating that initially the mobility of charge carriers generated in the oligomers would not be much affected by the presence of aromatic side groups, but the deposit would be very little conductive. This current decay could also be explained considering a charge intensity decrease associated to a p-doping process, as a result of an irregular deposit formation.

The difference between the electrodynamic profiles of both polymers might be due to MonA thiophene side groups that would promote twisting of PolyA central polymer chain, decreasing charge carrier mobility. This is evidenced by the shift, with respect to PolyB, of the initial oxidation potential toward more positive values. PolyB profile is much more alike to that of PANI, since MonB aniline groups are side units similar to o-substituted molecules, much less sterically hindered by the thiophene ring. However, the PolyB deposit would be much more irregular than that of PolyA since MonB possesses a greater number of active sites for growth.

### 3.2.7. Electronic properties

The magnitude of the bandgap  $E_g$  and frontier orbitals HOMO and LUMO energies are the most important features in determining the electrical and optical properties of a given conjugated polymer [32].

It is known that the oxidation onset potential  $(E_{on})^{ox}$ , corresponding to slope change of the anodic current in a cyclic voltammogram, correlates linearly with the frontier orbital energy HOMO ( $E_{HOMO}$ ). Likewise, there is a linear correlation between the reduction onset potential  $(E_{on})^{red}$  and the LUMO energy ( $E_{LUMO}$ ) [33]. This is mathematically expressed by the following equations:

$$E_{HOMO} = -((E_{on})^{ox} + 4.4) \text{ eV}$$

$$E_{LUMO} = -((E_{on})^{red} + 4.4) \text{ eV}$$

where the 4.4 value corresponds to a correction factor which applies to the formulas when the measured potentials are referred, as in this study, to the saturated calomel electrode.

Consequently, using electrochemical techniques the bandgap is possible to be determined as the difference between the HOMO and LUMO orbital energy of a conjugated polymer. However, the literature showed that certain electro-synthesized polymers, e.g. PANI derivatives, do not reveal their  $E_{LUMO}$ , because the reduction potentials lie outside the respective electrochemical window. In such cases UV-Vis spectroscopy studies are usually conducted. Spectra analysis enables  $E_g$  to be determined using the following equation:

$$E_{g_{opt}} = \frac{hc}{\lambda_{max}} = \frac{1242 \text{ eV}}{\lambda_{max}}$$

where  $\lambda_{\max}$  is the value of the intersection of the tangential through the inflection point of the absorption band of lower energy and higher intensity of the spectrum and the baseline set at  $y = 0$  [34].

Table 2 illustrates results of frontier orbitals energy and bandgap determined by electrochemical and optical techniques. Besides, data from reference [35] are also included about two typical electron acceptors: fullerene and PTCDA.

**Table 2.** PolyA and PolyB frontier orbital energy and bandgap.

Polymer	HOMO <sup>elec</sup> (eV)	LUMO <sup>elec</sup> (eV)	E <sub>g</sub> <sup>elec</sup> (eV)	E <sub>g</sub> <sup>opt</sup> (eV)
PolyA	5.6	3.7	1.9	2.1
PolyB	5.2	3.1	2.1	2.8
C <sub>60</sub>	-6.0	4.4	1.6	-
PTCDA	-6.9	4.8	2.1	-

As seen, differences between bandgaps calculated using electrochemical and optical methods exist. For PolyA the difference is small, because the polymer grows through a unique reactive center, namely the aniline unit. On the other hand, PolyB affords branched product, more disordered, due to the presence of two aniline units in the monomer, increasing thus the probability of growth sites, which directly affects the position of the energy level of the frontier orbitals. Furthermore, the measurement of electrochemical bandgap entails, among other experimental variables, effects associated to the nature of the supporting electrolyte and the type of electrode used, while the optical bandgap would be affected only by the type of solvent used and its value is usually more reliable.

If LUMO of the polymers compared with the typical materials used as electron acceptors in bilayer cells, e.g. fullerene C<sub>60</sub> and perylene-3,4,9,10-tetracarboxylic-dianhydride PTCDA, its difference is greater than 1 eV. This implies that charge transfer from the polymer photoexcited state into the conduction band of the acceptor compounds is possible. In addition, the HOMO energy of polymeric materials is higher than that of C<sub>60</sub> and PTCDA. According to Bernède [36], a compound can be classified as donor if presents HOMO and LUMO energy higher than that of the acceptor. Hence the prepared products exhibit properties, from the electronic point of view, suitable for photovoltaic cells fabrication.

Moreover, the synthesized polymers have an intermediate E<sub>g</sub> value with respect to PANI (4.5 eV) and PTh (2.1 eV), indicating that their electronic properties can be effectively combined and improved by preparing hybrid monomers.

### 3.2.8. Photovoltaic devices

Polymer deposition on different buffer layers was attempted in order to obtain the best possible efficiency of the device. The most appropriate was a MoO<sub>3</sub> layer. Different layer thicknesses were also tested. High series resistance were observed for thickness greater than 100 Å for PolyA and

greater than 200 Å for PolyB. This indicates that resistivity of PolyA is greater than that of PolyB, which, among other factors, would make a difference regarding to efficiency of photovoltaic devices.

Figure 8 and Table 3 summarize the results obtained after prototypes tests in the presence of sunlight. It is seen that short circuit current  $J_{sc}$  of both cells is low, which can be ascribed to polymers high resistivity as a result of structure branching (PolyB) or main chain torsion (PolyA). This kind of defects in the molecular geometry decreases electron delocalization, working against the intrachain charge carrier mobility. This is consistent with the results obtained from UV-Vis spectroscopy studies wherein no absorption above 700 nm, indicative of charge carrier delocalization, was observed. Besides, both polymers exhibit a distinct blue shift, revealing a modest conjugation.

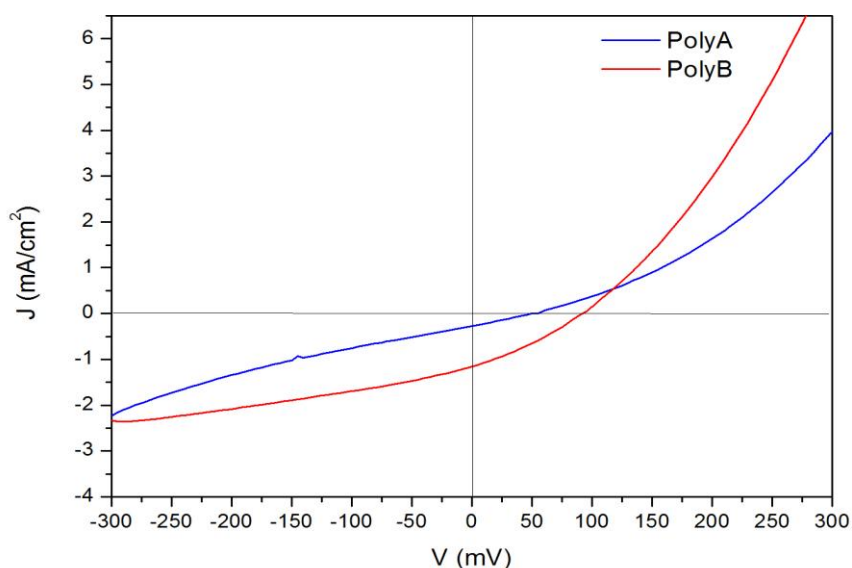


**Figure 8.** J-V characteristic of photocells prepared from PolyA and PolyB in presence of light.

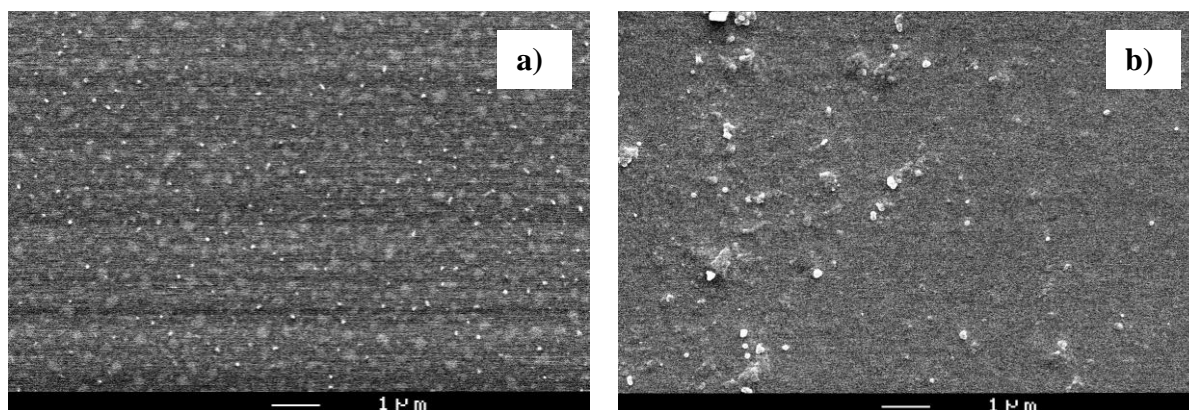


**Figure 9.** PolyA (a) and PolyB (b) SEM images

**Table 3.** Photocell electrical parameters

Polymer	$V_{oc}$ (V)	$J_{sc}$ (mA cm <sup>-2</sup> )	FF (%)	$\eta$ (%)
PolyA	50	0.28	26.30	$3.60 \cdot 10^{-3}$
PolyB	92	1.16	30.62	$3.26 \cdot 10^{-2}$

On the other hand, the packing of both polymers suggested they were mainly amorphous, with few or no crystalline regions, in agreement with the results obtained by differential scanning calorimetry, where no melting range was observed for the products. This amorphous packing produces a low  $J_{sc}$  and an interchain decrease of charge carrier transfer. At the same time, SEM data, Fig. 9, were collected. A chiefly smooth surface morphology of the products was observed. This would reveal a poor contact between the donor and the electron acceptor layers impairing the charge transfer between them and increasing cell reflectance [37-38]. The latter is just a hypothesis that is being checked by measuring the roughness at the donor/acceptor layer interface using AFM.

However, it has been assumed that the high resistivity of the polymers accounts for the poor efficiency of photovoltaic cells, revealing that the synthesized polymers, despite having suitable electrical properties, owing to their three-dimensional configuration are not appropriate for the suggested application. Nonetheless, to carry on working with the monomers as electron donor systems in copolymers containing a suitable acceptor chromophore group has not been ruled out.

#### 4. CONCLUSIONS

FT-IR and NMR studies showed that polymers growth occurs only through aniline unit(s), to give a linear product (PolyA) and a branched one (PolyB). No experimental evidence that thiophene units interact with the oxidizing agent was found. However, an electron donor effect, observable in UV-Vis spectra, would be exerted upon aniline units.

The novel polymers are sparingly soluble in typical organic solvents. However, due to their adequate thermal stability they can be also used for the fabrication of photovoltaic cells, since the polymers can be deposited by high vacuum sublimation. For this reason, estimation of their molecular size in solution is not as relevant, because during the sublimation process it has been shown that polymer chain cuts occurred.

Results obtained by electrochemical methods are consistent with those found from polymers structural characterization. In addition PolyA and PolyB present electronic properties suitable for use in organic solar cells and intermediate to those of PANIs and PThs. Unfortunately, due to the three-dimensional conformation they assume and their high resistivity, prototypes efficiency were of the order of  $10^{-2}$  and  $10^{-3}$ , which are quite poor. Despite this, is essential to demonstrate that electron donor monomers can be used in the preparation of copolymers with other chromophore electron acceptors to yield polymers with improved properties and higher photovoltaic efficiency.

## ACKNOWLEDGMENTS

Financial support through project FONDECYT 1095165 is kindly acknowledged. IAJ and PPZ thank CONICYT for a Doctoral Scholarship and Project ECOS/CONICYT C09E02.

## References

1. V. Prevost, A. Petit, F. Pla, *Eur. Polym. J.*, 35 (1999), 1229.
2. J. Desilvestro, W. Scheifele, O. Haas, *J. Electrochem. Soc.*, 139 (1992), 2727.
3. J. Joo, A.J. Epstein, *Appl. Phys. Lett.*, 65 (1994), 2278.
4. D. C. Trivedi, S. K. Dhawan, *Synth. Met.*, 59 (1993), 267.
5. W. K. Lu, R. L. Elsenbaumer, B. Wessling, *Synth. Met.*, 71 (1995), 2163.
6. M. Fahlman, S. Jasty, A.J. Epstein, *Synth. Met.*, 85 (1997), 1323.
7. F. R. Díaz, C. O. Sánchez, M. A. del Valle, L. H. Tagle, J. C. Bernède, Y. Tregouet, *Synth. Met.*, 92 (1998), 99.
8. M. A. del Valle, F. R. Díaz, M. E. Bodini, G. Alfonso, G. M. Soto, E. Borrego, *Polymer International*, 54 (2005), 526.
9. F. Brovelli, J. C. Bernède, S. Marsillac, C. Beadouin, F. R. Díaz, M. A. del Valle, *J. Appl. Polym. Sci.*, 86 (2002), 1128.
10. L. Torsi, A. Tafuri, N. Cioffi, M. C. Gallazzi, A. Sassella, L. Sabbatini, P. G. Zambonin, *Sens. Actuat. B Chem. B*, 93 (2003), 257.
11. M. R. Andersson, O. Thomas, W. Mammo, M. Svensson, M. Theander, O. Inganas, *J. Mater. Chem.*, 9 (1999), 1933.
12. D. T. McQuade, A. E. Pullen, T. M. Swager, *Chem. Rev.*, 100 (2000), 2537.
13. J. Liu, T. Tanaka, K. Sivula, A. P. Alivisatos, J. M. J. Frechet. *J. Am. Chem. Soc.*, 126 (2004), 6550.
14. S. Abaci, Y. Aslan, A. Yildiz, *J. Mat. Sci.*, 40 (2005), 1163.
15. Y. A. Udum, K. Pekmez, A. Yildiz, *J. Solid State Electrochem.*, 10 (2006), 110.
16. M. A. Abd El-Ghaffar, N. A. Mohamed, A. A. Ghoneim, *Polymer-Plastics Technology and Engineering*, 45 (2006), 1327.
17. O. Baudoin, D. Guénard, F. Guéritte, *J. Org. Chem.*, 65 (2000), 9268.
18. G. East, M. A. del Valle, *J. Chem. Ed.*, 77 (2000), 97.
19. N. Miyaura, T. Ishiyama, H. Sasaki, M. Ishikawa, M. Satoh, A. Suzuki, *J. Am. Chem. Soc.*, 111 (1989), 314.
20. A. E. Thompson, G. Hughes, A. S. Batsanov, M. R. Bryce, P. R. Parry, B. Tarbit, *J. Org. Chem.*, 70 (2005), 388.
21. S. C. NG, L. G. Xu, S. O. Chan, *J. Mat. Sci. Lett.*, 16 (1997), 1738.
22. F. Wudl, R.O. Angus, F.L. Lu, P.M. Allemand, D.J. Vachan, M. Nowak, Z.X. Liu, A.J. Heeger, *J. Am. Chem. Soc.*, 109 (1987), 3677.
23. A.A. Athawale, V.V. Chabukswar, *J. Appl. Polym. Sci.*, 79 (2001), 1994.
24. X. Wang, T. Sun, Ch. Wang, C. Wang, W. Zhang, Y. Wei, *Macromol. Chem. Phys.*, 211 (2010), 1814.
25. W. F. Alves, E. C. Venancio, F. L. Leite, D. H. F. Kanda, L. F. Malmonge, J. A. Malmonge, L. H. C. Mattoso, *Thermochimica Acta*, 502 (2010), 43.
26. V. Ballesterro, S. Carrara, *Langmuir*, 20 (2004), 969.
27. F. Geobaldo, G. T. Palomino, S. Bordiga, A. Zecchina, C. O. Areán, *Phys. Chem. Chem. Phys.*, 1 (1999), 561.
28. L. Dauginet-De Pra, S. Demoustier-Champagne, *Thin Solid Films*, 479 (2005), 321.
29. Lv. Rongguan, S. Zhang, *Synth. Met.*, 150 (2005), 115.
30. D. Shan, S. Mu, *Synth. Met.*, 126 (2002), 225.

31. Chen, W. C., Wen, T. C., Gopalan, A., *Journal of the Electrochemical Society*, 148 (2001), E427.
32. Y. J. Cheng, S. H. Yang, C. S. Hsu, *Chem. Rev.*, 109 (2009), 5868.
33. S. Admassie, O. Inganas, *Synth. Met.*, 156 (2006), 614.
34. D. A. M. Egbe, B. Cornelia, J. Nowotny, W. Günther, E. Klemm, *Macromolecules*, 36 (2003), 5459.
35. H. Dong, H. Zhu, Q. Meng, X. Gong, W. Hu, *Chem. Soc. Rev.*, 41 (2012), 1754.
36. J. C. Bernede, *J. Chil. Chem. Soc.*, 53 (2008), 1549.
37. H. Kim, M. Chandran, S. Park, H. Chae, J. Lee, Y. Choe, *Surf. Interface Anal*, 2012. DOI: 10.1002/sia.4988.
38. Z. Jehl, M. Bouttemy, D. Lincot, J. F. Guillemoles, I. Gerard, A. Etchberry. G. Voorwinden, M. Powalla, N. Naghavi, *J. Appl. Phys.*, 111 (2012), 114509.